frontiers | Frontiers in Earth Science

ORIGINAL RESEARCH
published: 24 May 2022
doi: 10.3389/feart.2022.873492

Contrasting Along-Slope vs. Downslope Sedimentation Style on the High-Latitude Eastern Canadian Continental Margin During the Last 40 ka

Harunur Rashid[1,2]*, *Jianing He*[1], *Ranjan Patro*[3] and *A. Owen Brown*[4]

[1]College of Marine Sciences, Shanghai Ocean University, Shanghai, China, [2]Earth and Environmental Sciences, Memorial University of Newfoundland, Corner Brook, NL, Canada, [3]College of the North Atlantic, St. John's, NL, Canada, [4]Geological Survey of Canada (Atlantic), Dartmouth, NS, Canada

Late Pleistocene Labrador Sea depositional systems developed in front of ice streams and glacier outlets from the Laurentide Ice Sheet (LIS) are documented by Huntec and 3.5 kHz seismic profiles and piston cores. Due to efficient grinding by the LIS, massive amounts of fine-grained sediments and meltwater in addition to the icebergs linked to the Heinrich events (H events) of the last glaciation were delivered to the neighboring Labrador Sea. The position of the Hudson Strait ice stream during the periodic expansion and contraction on the Labrador margin allowed fine-grained sediments and meltwater direct delivery on the lower shelf and upper slope. These discharges were then transported southward by the Labrador Current and western boundary current. In contrast to the lower shelf and upper slope, sediments delivered on the mid to the lower Labrador Slope were transported by the Northwest Atlantic Mid-Ocean Channel to distal sites. The nepheloid flow layer at or near the sea bottom or at mid-water depths developed from meltwater loaded with an excessive charge of fine-grained sediments. Contrastingly, the non-discriminatory ice rafting process delivered detritus of all sizes, but its total contribution to the sediment column was only minor, notwithstanding its paleoclimatic significance during H events. Heinrich H1, H2, and H4 layers were identified by their characteristic nepheloid flow layer deposits, that is, alternating coarse silt and clay-sized laminae with thin ice-rafted debris interspersed by coarse- to fine-grained dropstone. Furthermore, the progressive thinning and eventual disappearance of the fine-laminae (i.e., coarse and fine silt/clay) in H layers at the distal sites suggest the exhaustion and raining out of fines due to long-distance transport. However, the H3 layer was identified by a combination of nepheloid flow layer deposits (upper slope) and finely laminated mud turbidites (lower slope and deep basin) at proximal sites. In the lower Labrador Slope and Basin, the H3 stratigraphic equivalent layer was identified by exorbitantly thick finely laminated carbonate-rich mud turbidites. The divergent sedimentation style (i.e., reflected by the sediment facies) and the thickness of the H3 layer compared to other H events suggest that the Hudson Strait ice stream position was different from other H events. Therefore, our data imply that the divergence in the H3 layer between the eastern and western North Atlantic might lie with the position of the Hudson Strait ice stream on the Labrador continental margin.

Keywords: sediment dynamics, Heinrich events, nepheloid-layer flow deposits, mud turbidites, Labrador Sea, Holocene, Last Glaciation

OPEN ACCESS

Edited by:
Daidu Fan,
Tongji University, China

Reviewed by:
Rong Wang,
Ministry of Natural Resources, China
Matt O'Regan,
Stockholm University, Sweden

***Correspondence:**
Harunur Rashid
Harunurbhola@gmail.com

Specialty section:
This article was submitted to Marine Geoscience, a section of the journal Frontiers in Earth Science

Received: *10 February 2022*
Accepted: *11 April 2022*
Published: *24 May 2022*

Citation:
Rashid H, He J, Patro R and Brown AO (2022) Contrasting Along-Slope vs. Downslope Sedimentation Style on the High-Latitude Eastern Canadian Continental Margin During the Last 40 ka. Front. Earth Sci. 10:873492. doi: 10.3389/feart.2022.873492

1 INTRODUCTION

Continental shelves of the eastern Canadian margin are >100 km wide and underlain by a wedge of Mesozoic and Cenozoic clastic sedimentary rocks. Almost the entire continental shelf off eastern Canada has been glaciated numerous times in the mid to late Pleistocene, resulting in transverse troughs and intervening banks. A powerful south-flowing surface Labrador Current, most vigorous at times of high freshwater input to the Labrador Sea (Lazier and Wright, 1993), sweeping the continental shelf break along the southeastern Canadian margin. Deepwater circulation forms the western boundary current (WBC) flows at >2.5 km water depth on the Labrador Rise, more vigorous at times of greater deepwater production, for example, during interglacials. Seaward of Hudson Strait, detailed studies by earlier researchers, has made this a type area for understanding discharges seaward of ice streams (Andrews and Tedesco, 1992; Maclean, 2001; Andrews and MacLean, 2003; Rashid and Piper, 2007). The discharge is rich in detrital carbonates, known as the Heinrich iceberg rafting events (H events) or detrital carbonate events (DC events), making it easy to trace in the adjacent ocean. The continental slope off Hudson Strait is underlain by glacigenic debris flows, the youngest dating from about 30 cal. ka (Rashid and Piper, 2007; Rashid et al., 2019a). The dynamics of fine sediment deposition on the continental slope and rise from meltwater discharge have been elucidated (Hesse et al., 2004). Sediment lofting from turbidity currents shows a vital process in proximal slope areas (Hesse and Khodabakhsh, 2006); hypopycnal plumes associated with meltwater discharge from the Hudson Strait ice stream must be responsible for deposition on the continental shelf, and icebergs rafting is important (Dowdeswell et al., 1995; Rashid et al., 2003a; Rashid et al., 2017). Fine-grained carbonate-rich turbidites overlie many H layers in the Labrador Sea, most notably in H3 (Rashid et al., 2003a; Rashid et al., 2003b; Rashid et al., 2019a).

One of the notable sediment events that captured the imagination of marine geoscientists and paleo-climatologists over the last three decades is the H events and their direct relationship to the dynamics of ice sheets surrounding the North Atlantic during the last glacial cycle (Bond et al., 1993; Hillaire-Marcel et al., 1994; Dalton et al., 2022; and references therein). The rich literature on H events (Cf. Dalton et al., 2022; Andrews and Voelker, 2018; and references therein) state that Heinrich (1988) provided the first account of six iceberg rafting events (H events) during the last glaciation from the Dreizac seamounts of the NE Atlantic. Subsequently, Bond et al. (1993) correlated H events to broad atmospheric and sea surface temperature changes in the North Atlantic and the surrounding regions and connected H events to global climate changes. However, the recent uptick of interest in H events (e.g., Velay-Vitow et al., 2020; Condron and Hill, 2021; Zhou et al., 2021) and their link to the sediment delivery mechanisms, especially from the NW Atlantic, including the Labrador Sea deserve further detailing and clarification. For example, using a high-resolution seafloor mapping from Cape Hatteras (~35°N) and Florida Keys (~24°N) and piston cores from North Carolina Slope, Condron and Hill (2021) reported Hudson Strait sourced icebergs for the H3 layer. In addition, the authors used a dynamic–thermodynamic iceberg and Massachusetts Institute of Technology general circulation models results to propose the transport of icebergs and meltwater along the entire eastern seaboard of the United States as far south as Florida Keys (~24°N). It is unclear what mechanisms would have impeded iceberg melting, given the high temperature at ~24°N of the subtropical North Atlantic. Using a suite of sediment cores in conjunction with the multibeam bathymetry and Huntec and 3.5 kHz seismic profiles, Rashid et al. (2017); Rashid et al. (2019b) documented H events including the H3 layer and other fast sediment events on the SE Grand Banks and Newfoundland Basin. The authors further delineated sediment deposits along the slope (i.e., long-distance transport) vs. downslope transport. In a rather dramatic finding, Dalton et al. (2019) proposed that the Hudson Strait ice stream retreated landward from its position on the Hatton Basin during H4 time to immediately H3 time, implying an ice-free Hudson Strait, which was contradicted by Miller et al. (2019). Yet the past records from the Hudson Strait and surrounding regions suggest an extension of the Hudson Strait ice stream as far offshore as the Hatton Basin (Andrews and MacLean, 2003; Rashid and Piper, 2007). Moreover, using a global ocean model in which tidal forcing was used to assess the instability of the ice sheets surrounding the North Atlantic, Velay-Vitow et al. (2020) proposed that the Laurentide ice sheet was rendered unstable by the high-amplitude M2 tide at the time of H3. Despite the recent findings for H3 and H4 layers, the sedimentological aspects (i.e., sediment transport and meltwater discharge) in and around the Hudson Strait ice stream are inadequately understood. Therefore, this study is designed to 1) re-assess the dynamics of the Hudson Strait ice stream during the past 40 ka using new high-resolution (Huntec) seismic profiles and sediment cores and partially published records, 2) attempt to reconcile the conflicting interpretation between along slope and downslope sedimentation style during H3 and H4 events, and 3) assess the mode of sediment transport during the Holocene and last glaciation on the Labrador continental margin.

2 MATERIALS AND METHODS

2.1 Sediment Cores From the NW Labrador Sea off Hudson Strait

Calypso piston core **MD99-2233** (hereafter 33) was retrieved from the lower Labrador Slope (**Figure 1A**), immediately south of the Hudson Strait ice stream, during the IMAGES MD1999 cruise. It was collected at 2350 m water depth, and it is 2462 cm long. Some of the data from core 33 were published in Rashid et al. (2003b) and Rashid and Piper (2007); however, new findings are brought to light incorporating sediment physical properties and deep-tow Huntec seismic profile in addition to the sediment geochemistry and ^{14}C-AMS dates.

Piston core **Hu2006040-47** (hereafter 47) was collected on the Saglek Bank from the Labrador Slope at 2049 m water depth, and it is 20 km south and ~300 m shallower water than core 33. The smooth sea bottom surface that appeared in the deep-tow Huntec seismic profile (Campbell, 2007) suggests a lack of apparent surface disturbance. Core 47 is 883 cm long, and its records are reported here for the first time.

2.2 Nain Bank and Hamilton Bank Sediment Cores

Piston core **Hu2006040-58** (hereafter 58) was collected from the Nain Bank on the lower Labrador Slope at 1999 m water depth. The core was retrieved from a strategic location to assess pathways for sediment plume and iceberg discharge originating from the Hudson Strait ice stream and any sediment supply from the Okak Trough on the Labrador Shelf. It is 734 cm long, and the data from this core are reported here for the first time.

Core **Hu2006040-06** (hereafter 06) was collected from the Hamilton Spur of the Hamilton Bank on the upper Labrador Slope at 736 m water depth. Deep-tow Huntec seismic profile reflects the lack of identifiable sea bottom disturbances or iceberg scouring. Core 06 is 784 cm long; however, the top 410 cm is used for this study. Core 06 is chosen to assess the extent to which sediment plumes can be traced from the Hudson Strait on the Labrador Slope.

2.3 Deep Labrador Basin Sediment Cores From the Eastern Northwest Atlantic Mid-Ocean Channel Levee

Core **MD99-2226** (hereafter 26) was raised by the Calypso corer under the IMAGES program (Hillaire-Marcel et al., 1999) from the eastern levee of the Northwest Atlantic Mid-Ocean Channel (NAMOC); **Figure 1B** at 3,580 m water depth. Core 26 was chosen to assess whether mass transport deposits originating from deep water off the Hudson Strait ice stream can be traced to the distal site. The Holocene section of the records spanning the upper 125 cm was published in

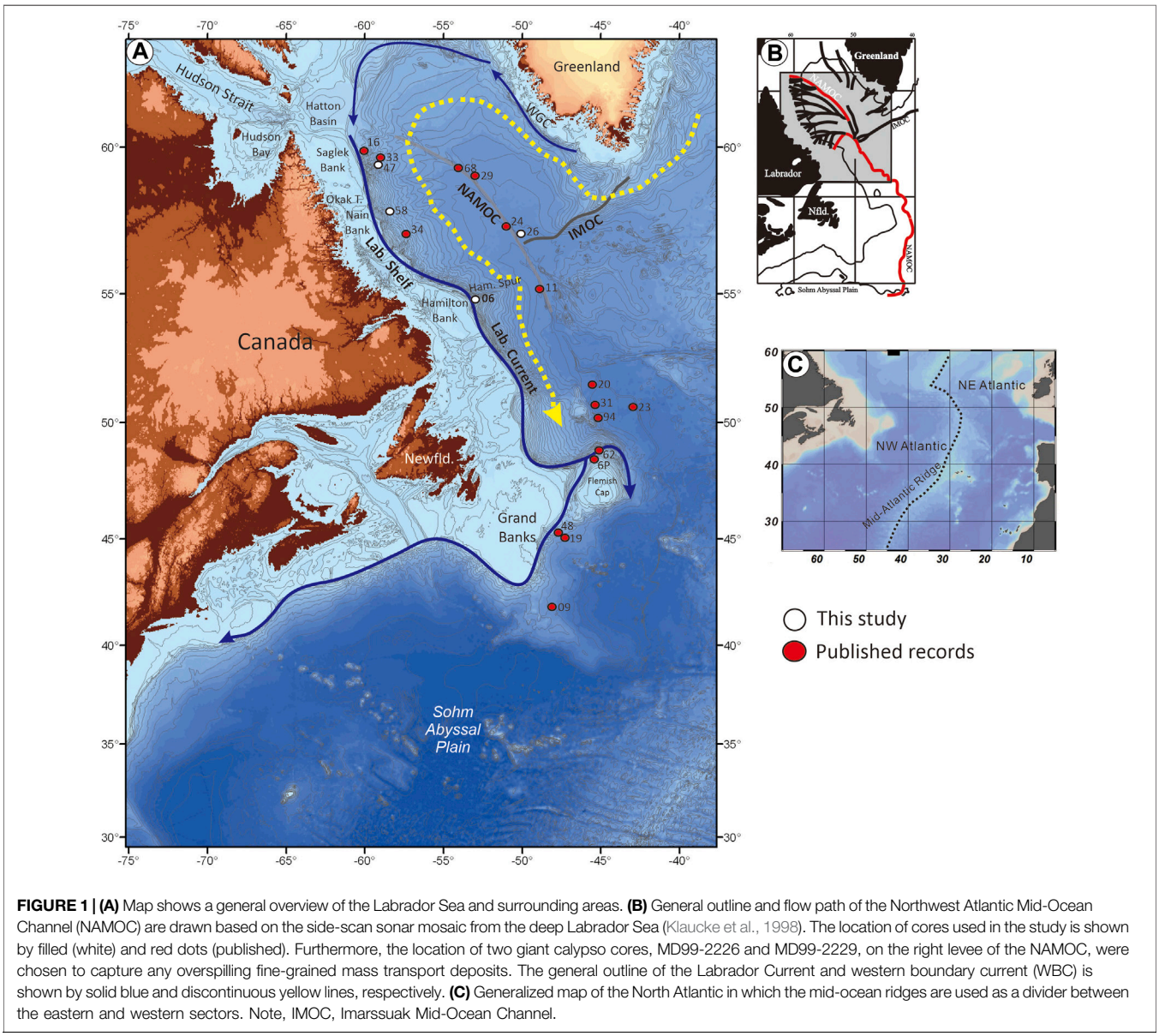

FIGURE 1 | (A) Map shows a general overview of the Labrador Sea and surrounding areas. **(B)** General outline and flow path of the Northwest Atlantic Mid-Ocean Channel (NAMOC) are drawn based on the side-scan sonar mosaic from the deep Labrador Sea (Klaucke et al., 1998). The location of cores used in the study is shown by filled (white) and red dots (published). Furthermore, the location of two giant calypso cores, MD99-2226 and MD99-2229, on the right levee of the NAMOC, were chosen to capture any overspilling fine-grained mass transport deposits. The general outline of the Labrador Current and western boundary current (WBC) is shown by solid blue and discontinuous yellow lines, respectively. **(C)** Generalized map of the North Atlantic in which the mid-ocean ridges are used as a divider between the eastern and western sectors. Note, IMOC, Imarssuak Mid-Ocean Channel.

Rashid et al. (2014). However, core 26 is 3,214 cm long, and it is chosen to assess the movement of the mass transport deposit by the NAMOC (**Figure 1B**) in the deep Labrador Basin. Furthermore, core **MD99-2229** (hereafter 29) is 3,628 cm long at 3,400 m water depth and was collected 274 km upstream of core 26. The locations of cores 26 and 29 have been placed within the side-scan sonar imagery and swath bathymetry (acquired by Hawaii Institute of Geophysics Acoustic Wide-Angle Imaging Instrument Mapping Researcher 1; HAWAII MR-1; Klaücke, 1995; Rashid et al., 2019a). The sediment records of core 29 are chosen to complement the records of core 26.

Sediment cores collected during the Hu2006040 cruise (Campbell, 2007) have Huntec or 3.5 kHz seismic profile near or through the core sites. However, the 3.5 kHz seismic profile at site 29 was lost due to technical problems during the MD1999 cruise. In any event, most of the cores used in the study have a good seismic stratigraphy; thus, the combination of seismic profile and piston core provides a window to the near-surface sea bottom geomorphology and whether the core site possesses any mass transport deposits (i.e., glacigenic debris flow and turbidites) on the Labrador margin (Rashid and Piper, 2007; Rashid et al., 2019a).

Sediment physical properties, namely, magnetic susceptibility, compressional (P) wave velocity, bulk, and density, were acquired at 2-cm intervals using the GeoTek MSCL system onboard 1999 Marion Dufresne (MD 1999) for cores 26, 29, and 33. An MSCL system was used to measure P-wave velocity, bulk density, and magnetic susceptibility for cores 06, 47, and 58 at the Geological Survey of Canada (Atlantic; GSC-A). X-radiographs of 1-cm thin sediment slabs of cores 26, 29, and 33 were used to identify sediment facies, whereas the whole-core X-ray is available for cores 06, 47, and 58. Wet sediment surface color (L, a*, and b*) was determined at 5-cm intervals on a 1-cm-diameter spot using a handheld digital spectrophotometer (Minolta CM-2002) from core splits onboard the MD1999 cruise. An identical digital spectrophotometer and setup were used to obtain sediment color at 1-cm intervals of cores 06, 47, and 58 on the wet sediment surface using a Saran wrap at the GSC-A.

Bulk sediment carbonate concentration (expressed as % $CaCO_3$) of core 33 was determined using a LECO WR-112 carbon analyzer at the GSC-A (Rashid and Piper, 2007). Contrastingly, the bulk sediment geochemistry of cores 26 and 47 was inferred using an Innov-X DELTA Premium (DP-6000) portable X-ray fluorescence (pXRF) core scanner at 1-cm intervals. The semiquantitative concentration of 25 elements was determined; however, the Ca/Ti, Zr/Ti, and Rb/Ti ratios in conjunction with sediment physical properties were used to identify sediment sources, Heinrich (H) layers, and other stratigraphic markers in this study (Rashid et al., 2019a). The Ca/Ti ratios are successfully correlated to the detrital carbonate (i.e., % $CaCO_3$) concentration of the bulk sediments, whereas the Zr/Ti and Rb/Ti ratios are often used as proxies for sand (Cuven et al., 2010) and terrestrial output to the Labrador Sea (Piper et al., 2021).

Based on the physical properties, X-radiographs, and core photographs, 24 sediment horizons were chosen to pick foraminifera for age dating. Approximately 5 mg of polar planktonic foraminifera *Neogloboquadrina pachyderma* were picked using a binocular microscope. A total of 24 samples (**Table 1**) were sent to the Keck Carbon Cycle Laboratory at the University of California in Irvine and Andre Lalonde AMS Laboratory at the University of Ottawa for ^{14}C-AMS dating. ^{14}C-AMS dates were calibrated using the Calib 8.10 program (Reimer et al., 2020) by applying the Marine20 reservoir (Heaton et al., 2020) curve. The Calib 8.1 incorporated 550 years for marine reservoir age (R) by the latest iteration of the IntCal20 (Reimer et al., 2020), which was applied to this study. A regional reservoir age (ΔR) of 50 years is also applied. It should be stated a priori that the choice of R or ΔR in calibrating the ^{14}C-AMS dates for the study has no bearing on our identification of H layers.

3 RESULTS AND INTERPRETATION

Identification of H layers in this study was carried out mostly following the published criteria, including sediment facies (**Table 2**) specific to the NW Labrador Sea detailed by Hesse and Khodabakhsh (1998) and Rashid et al. (2003a); Rashid et al. (2019a). However, differences exist in sediment facies in H layers between the proximal sites such as off Hudson Strait than those of the distal sites on the northern Flemish Pass slope and SE Grand Banks, which are detailed in the discussion. In any event, H1, H2, and H4 layers are identified in cores 33, 47, 58, and 06 (**Figures 2–5**) by the nepheloid flow layer sediment facies (i.e., alternating coarse silt and clay-sized laminae with thin ice-rafted debris interspersed by coarse- to fine-grained dropstones) in conjunction with high L* and a*-trace, Ca/Ti ratios, low magnetic susceptibility, high density, and P-wave velocity.

The covariation between the L*-parameters and %$CaCO_3$ in the bulk sediments (**Figure 2**) in which high %$CaCO_3$ matches with high L*values in core 33 and is considered an increase in the detrital carbonates sourced from the late Paleozoic carbonate rocks flooring the Hudson Bay and Hudson Strait (Andrews et al., 1993; MacLean, 2001; Rashid et al., 2003a). Hesse and Khodbakhsh (1998) and Rashid et al. (2003a), Rashid et al. (2019a) demonstrated that the high % $CaCO_3$ values in the NW Labrador Sea sediment cores, often correlated to the H layers, are mostly detrital carbonates. This strong covariation between the L*-values and high %$CaCO_3$ was used as an index for high detrital carbonates in cores, in which % $CaCO_3$ data are lacking.

The interval representing the Holocene period is identified by their olive-green (proximal to slope) to olive-gray (deep basin) hemipelagic sediments with or without IRD sediment facies. The thickness of the Holocene interval on the Labrador Slope varies from ~5 cm in core 33 (**Figure 2**) on the Saglek Bank to 20 cm in core 06 (**Figure 4**) on the Hamilton Spur. However, the Holocene interval in core 26 (**Figure 6A**) is relatively thick at 125 cm (Rashid et al., 2014), consistent with the broader Labrador Basin sedimentation pattern (Hoogakker et al., 2014).

H1, H2, H3, and H4 layers in core 33 (**Figure 2**) were identified from 45 to 200 cm, 400–560 cm, 812–1,480 cm, and 1,525–1,642 cm subsurface depths, respectively. Six ^{14}C-AMS dates aided this identification (Rashid et al., 2003b; Rashid and Piper, 2007). Parallel-laminated fine-grained detrital carbonates rich mud turbidites between 260 and 320 cm separated by the hemipelagic sediments with IRD at the top and bottom are deemed to be unrelated to H layers. The deposition of this

TABLE 1 | ^{14}C-AMS dates used in the study.

	Core	Depth (cm)	^{14}C-AMS dates	Materials dated	Calibration age ±1σ (years)	Median age (years)	References
1	MD99-2233	210	14,320 ± 170	*N. pachyderma*	16,186–16,678	16,434	Rashid et al. (2003a)
2	MD99-2233	330	18,600 ± 160	*N. pachyderma*	21,368–21,854	21,600	Rashid et al. (2003a)
3	MD99-2233	380	19,950 ± 110	*N. pachyderma*	22,912–23,221	23,073	Rashid et al. (2003a)
4	MD99-2233	790	22,450 ± 190	*N. pachyderma*	25,618–26,004	25,817	Rashid et al. (2003a)
5	MD99-2233	1,500	26,700 ± 370	*N. pachyderma*	29,701–30,489	30,074	Rashid et al. (2003b)
6	MD99-2233	1,640	35,800 ± 300	*N. pachyderma*	39,623–40,228	39,929	Rashid et al. (2003b)
7	Hu2006040-47	234–236	17,555 ± 45	*N. pachyderma*	20,185–20,419	20,299	St-Ange et al. (2013)
8	Hu2006040-47	431–434	25,420 ± 260	*N. pachyderma*	28,522–29,075	28,778	St-Ange et al. (2013)
9	Hu2006040-47	819–821	27,650 ± 240	*N. pachyderma*	30,736–31,145	30,935	St-Ange et al. (2013)
10	Hu2006040-58	450–452	19,610 ± 45	*N. pachyderma*	22,593–22,846	22,711	This study
11	Hu2006040-58	550–552	22,050 ± 60	*N. pachyderma*	25,324–25,592	25,454	This study
12	Hu2006040-06	161–162	15,675 ± 40	*N. pachyderma*	18,039–18,234	18,135	This study
13	Hu2006040-06	270	22,160 ± 110	*N. pachyderma*	25,408–25,718	25,558	Hoffman (2016)
14	Hu2006040-06	410–411	28,310 ± 180	*N. pachyderma*	31,266–31,674	31,486	This study
15	MD99-2226	50–51	6,920 ± 30	*N. pachyderma*	7,163–7,306	7,239	Rashid et al. (2014)
16	MD99-2226	127–128	9,140 ± 660	*N. pachyderma*	8,876–10,599	9,762	Rashid et al. (2014)
17	MD99-2226	2598–2600	42,073 ± 650	*N. pachyderma*	43,484–44,570	44,050	This study
18	MD99-2226	3,198–3,200	46,633±1,108	*N. pachyderma*	46,972–49,686	48,422	This study
19	MD99-2226	3,190–3,195	46,900 ± 810	*N. pachyderma*	47,660–49,665	48,654	This study
20	MD99-2229	125	20,500 ± 90	*N. pachyderma*	23,548–23,835	23,694	Rashid et al. (2019a)
21	MD99-2229	195	24,200 ± 110	*N. pachyderma*	27,383–27,650	27,514	Rashid et al. (2019a)
22	MD99-2229	1,481	30,400 ± 340	*N. pachyderma*	33,742–34,393	34,058	Rashid et al. (2019a)
23	MD99-2229	1,501	33,360 ± 480	*N. pachyderma*	36,432–37,730	37,170	Rashid et al. (2019a)
24	MD99-2229	2585–2595	>42,000	*N. pachyderma*			Rashid et al. (2019a)

TABLE 2 | Sediment facies identified and used in the study.

Facies name	Characteristic features	Interpretation	Detailed description in
1	Nepheloid flow layer (brown to beige color)	Continental margin and deep Labrador Basin	Rashid et al. (2003a), Rashid et al. (2012); this paper
2	Turbidites	Deep marine	Rashid and Piper (2007); Wang and Hesse (1996); this paper
3a	Olive gray sandy mud (sediments)	Marine (hemipelagic), proximal to Labrador Shelf	Rashid et al. (2012); this paper
3b	Olive gray sediments	Marine (hemipelagic), deep Labrador Basin	Rashid et al. (2003b); this paper
4a	Olive green sediments with IRD	Glacio-marine, proximal to Labrador Shelf	Rashid et al. (2012); this paper
4b	Olive gray sediments with IRD	Glacio-marine, deep Labrador Basin	Rashid et al. (2003b); this paper
5	Greenish-gray mud, massive	Holocene-marine, proximal to Labrador Shelf	This paper
6	Brown mud, mottled with clasts	Holocene-marine, proximal to Labrador Shelf	This paper

turbiditic sediment unit (i.e., 260–320 cm) is most likely related to local mass transport due to the regional absence of an equivalent sediment unit.

Core 47 contains H1, H2, and H3 layers between 105 and 168 cm, 285 and 392 cm, and 450 and 810 cm subsurface depths (**Figure 3**), respectively, which were confirmed by three ^{14}C-AMS dates. Using the back counting method, the high L* and a*trace with high Ca/Ti ratios between 55 and 72 cm devoid of typical nepheloid flow layer deposits most likely represent the H0 layer (Andrews et al., 1995; Rashid et al., 2011; Rashid et al., 2019a).

On the Nain Bank in core 58, H1 and H2 layers were identified from 362 to 415 cm and 488–528 cm subsurface depths (**Figure 4**). Two ^{14}C-AMS dates at 450–452 and 550–552 cm confirm the identification of H1 and H2 layers. Moreover, the interval between 630 and 720 cm with high physical properties and high L* and a*trace most likely represents the top part of the H3 layer. It is apparent that the entire H3-layer was not cored due to incomplete recovery. The interval between the core top and 142 cm most likely represents the deglacial period or early Holocene (Jennings et al., 2015), which cannot be constrained due to the lack of ^{14}C-AMS dates at present.

H1, H2, and H3 layers in core 06 were identified between 145 and 158 cm, 248 and 269 cm, and 285 and 400 cm subsurface depths (**Figure 5**), respectively, which were confirmed by three ^{14}C-AMS dates (**Table 1**). Using the back counting method, the high L* and a*trace with high Ca/Ti ratios between 103 and 108 cm most likely represent the H0 layer (Rashid et al., 2011; Rashid et al., 2019a; Jennings et al., 2015) on the Hamilton Spur.

H3 and H4 equivalent sediment layers were identified by the parallel-laminated detrital carbonate-rich mud turbidites in two deep Labrador Basin cores, that is, 26 and 29. The thickness of H3 and H4 equivalent layers varies from 800 to 1,500 cm, which is exorbitantly thick compared to the nepheloid flow layer deposits identified by H

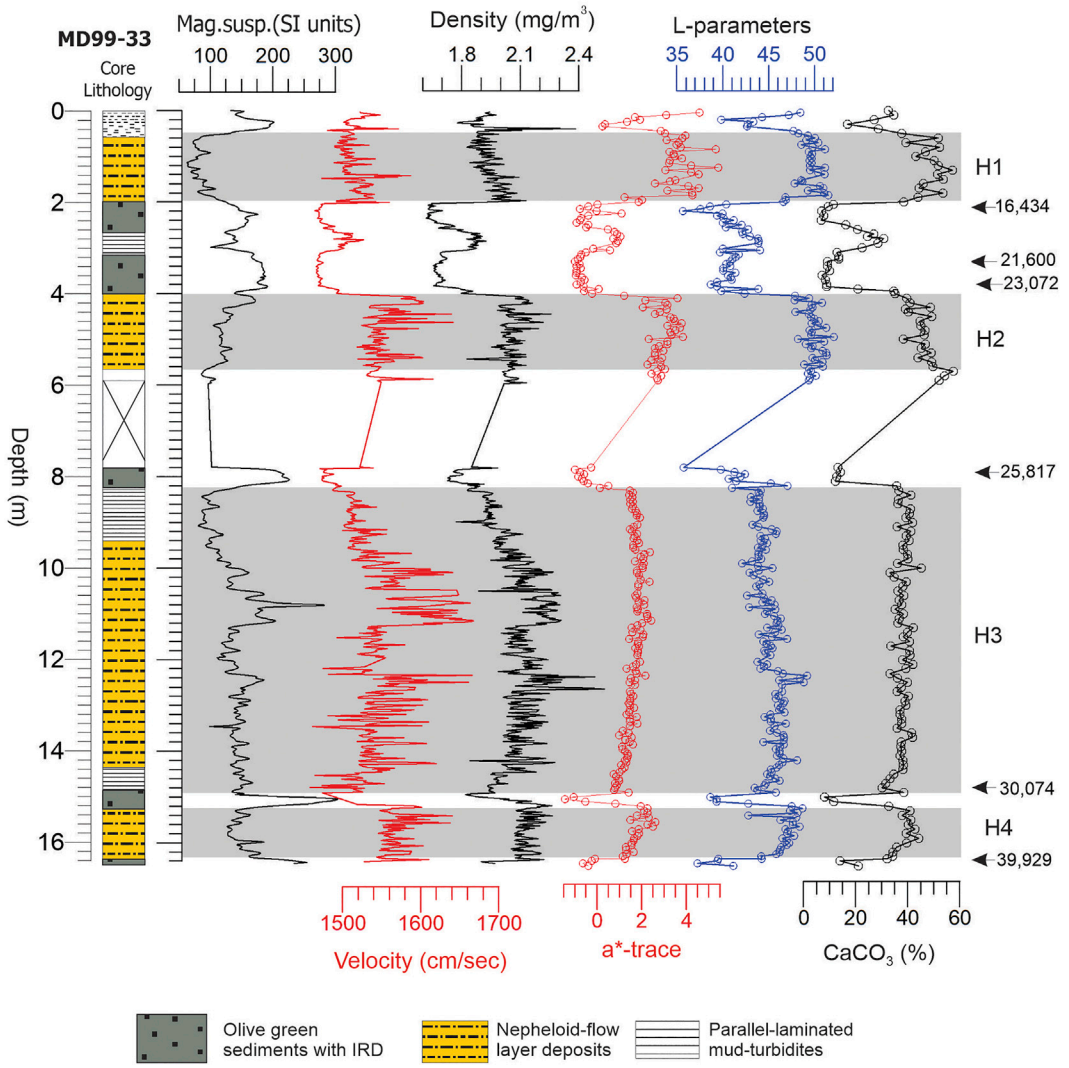

FIGURE 2 | Sediment physical properties, namely, magnetic susceptibility, P-wave velocity and density, sediment color a*-trace and L*, and $CaCO_3$ (%) in the bulk sediments, in addition to core photographs and X-radiographs, were used to assign sediment facies of core MD99-2233 shown in column (a). Six ^{14}C-AMS dates, which were converted to calendar years using the CALIB 8.10, are shown by the black horizontal arrows. H1, H2, H3, and H4 layers are identified by their typical nepheloid flow layer facies and detrital carbonate (reflected by $\%CaCO_3$), constrained by the ^{14}C-AMS dates.

layers (**Figures 2–5**). Three ^{14}C-AMS dates of core 29 confirm the identification of H3 equivalent layer between 220 and 1,400 cm subsurface depth (**Figure 6B**). Two ^{14}C-AMS dates at 3,190–3,195 and 3,198–3,200 cm (**Table 1**) in core 26 suggest that the parallel-laminated mud turbidites between 2600 and 3,120 cm are most likely H5 equivalent layer. Furthermore, the interval between 930 and 2595 cm and a ^{14}C-AMS date at 2598–2600 cm in core 26 suggests that they might contain H3 and H4 equivalent layers. The sudden increase in density between 2070 and 2450 cm (**Figure 6A**) and the fluctuating in velocities between 1,630 and 2070 cm (**Figure 6A**) are similar to those flickering in velocities between 1,680 and 1720 cm, that is, toward the top of H4 equivalent layer of core 29. Therefore, it is hypothesized that the interval between 930 and 1,630 cm is most likely an H3 equivalent layer, which needs to be independently confirmed by obtaining ^{14}C-AMS dates between 1,620 and 1,630 cm.

4 DISCUSSION

4.1 Sedimentation Style Between the Last Glaciation and Holocene on the Labrador Margin

The position in the eastern sector ice margin of the LIS and glacier outlets determined the sediment dynamics and meltwater discharge to the NW Atlantic, including the Labrador Sea, during the last glaciation (Margold et al., 2016; Dalton et al., 2022). Due to the expansion of the LIS during the last glaciation, the ice margin on the NE sector most likely crossed the continental shelf and extended to the upper Labrador Slope (MacLean, 2001; Andrews and MacLean, 2003; Rashid et al., 2019a). Furthermore, the Hudson Strait ice stream may have extended to the outer Hatton Basin,

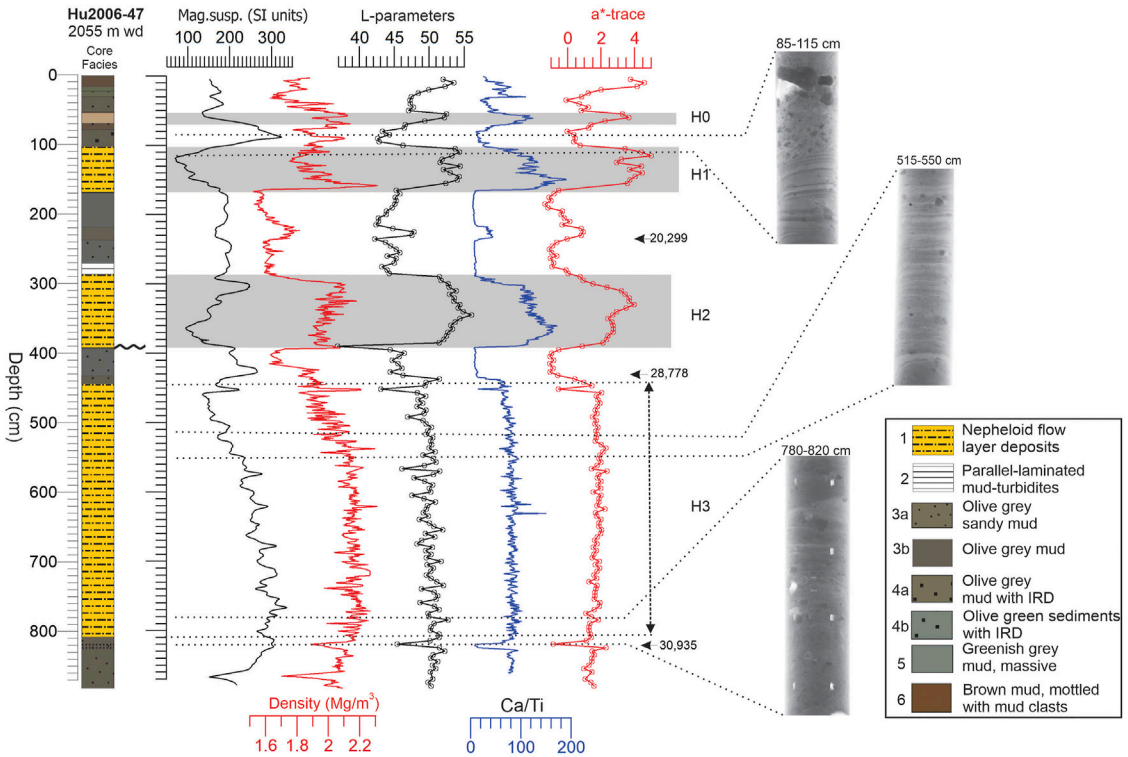

FIGURE 3 | Magnetic susceptibility and density of bulk sediments, sediment color L*, Ca/Ti ratios, a*-trace, X-radiographs, and core photographs were combined to assign sediment facies of core Hu2006040-47. Three ^{14}C-AMS dates, shown by black arrows, ascertain the identification of H1 and H2 layers between 102 and 168 cm and 286 and 392 cm, respectively. Three representative X-radiographs show sedimentary structures of H2, and H3 layers (515–550 cm and 780–820 cm) are also illustrated on the right.

resulting in meltwater supply and fine-grained sediments discharged directly on the Labrador Slope (Rashid and Piper, 2007; Dalton et al., 2021). This physical imposition on the NE ice margin set the stage for sediment delivery and iceberg supply during the periodic collapses accompanying H events (Andrews and Tedesco, 1992; Rashid et al., 2003a; Margold et al., 2018; Bassis et al., 2017), as illustrated in **Figures 2–5**. Furthermore, using 3.5 kHz seismic profiles and ground-truthing piston cores, Rashid and Piper (2007) demonstrated the position of the ice margin on the Labrador Shelf and Shelf edge during H3, H2, and H1. However, the ice margin position could not be constrained during H4 or earlier periods due simply to the erosive nature of the seismic reflector labeled as "III" (see Figure 6 of Rashid and Piper, 2007). This erosional seismic marker may suggest complete erosion of earlier deposited sediments above the Tertiary unconformity. There is also evidence of ice margin advance and extensive shelf glaciation on central–western Greenland, across the Hudson Strait ice stream on the Labrador Sea during MIS4 (Seidenkrantz et al., 2019). This extensive glaciation on the central–western Greenland ice margin might imply a similar advance of the Hudson Strait ice stream. In sum, the ice margin extension of the LIS and Hudson Strait ice stream on the Shelf and Shelf edge during the last glaciation starved the vast Labrador continental Shelf stretching from Saglek Bank to the Hamilton Spur (Josenhans et al., 1986; Rashid et al., 2017; Lochte et al., 2020).

In contrast to the last glacial period in which sediment and meltwater were delivered on the lower continental Shelf and upper Slope, the stepwise retreat of the LIS ice margin during the last deglaciation and early Holocene profoundly changed the sediment and meltwater discharge to the upper Shelf (Josenhans et al., 1986). The very thin or absence of Holocene sediments in cores 33, 47, 58, and 06 (**Figures 2–5**) reflect such changes in the sedimentation regime. Changes in the LIS ice margin configuration also had a profound bearing on the interactions among various surface currents and meltwater supply from the Canadian Arctic Archipelago (Gibb et al., 2015; Rashid et al., 2017; Lochte et al., 2020). After the physiographic imposition of the LIS ice margin (Dalton et al., 2021; Margold et al., 2018) was gradually removed starting at ~14 ka, the entire Labrador Shelf received sediments and meltwater due to the melting of the ice sheet, the opening of Tyrrell Sea, noble inlet advancement and retreat, and the final Lake Agassiz–Ojibway drainage (Barber et al., 1999; Matero et al., 2017). Some of these discharge events supplied an adequate amount of fine-grained sediments within the sediment plume to be transported at site 06 (**Figure 4**) on the Hamilton Spur. These periodic supplies of Hudson Strait and other minor sourced sediments and meltwater from the Labrador Shelf were also reported in numerous sediment records on the Saglek Bank

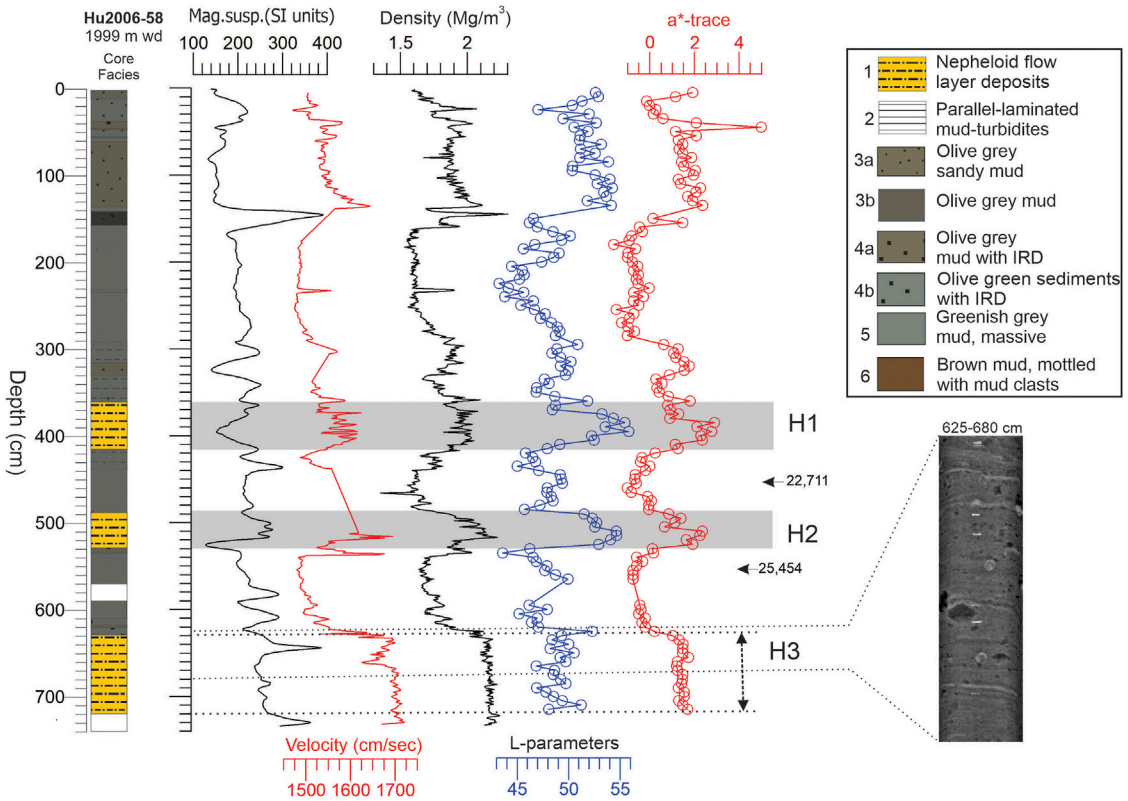

FIGURE 4 | Magnetic susceptibility, P-wave velocity, and density of the bulk sediments, L* and a*-traces, X-radiographs, and core photographs were used to assign sediment facies of core Hu2006040-58. H1 and H2 layers are identified between 362 and 415 cm and 482 and 526 cm by two ^{14}C-AMS dates. The interval between 630 and 715 cm is most likely the H3 layer. A representative X-radiograph of the H3 layer between 625 and 680 cm demonstrates the waning influence of sediment plume, ~1,000 km distance from the Hudson Strait ice stream at site 58.

(Rashid et al., 2017; Lochte et al., 2020), Cartwright Saddle (Hillaire-Marcel et al., 2007; Jennings et al., 2015), Notre Dame Trough (Roger et al., 2013), and northern Flemish Cap (Piper et al., 2021). These sediments appeared to be carried within the sediment plume and icebergs upstream by the Baffin Island and Labrador Currents (Rashid et al., 2019b; Piper et al., 2021). Furthermore, the intensification of the WBC during the Holocene may have also winnowed the already thin Holocene layer in deeper water cores (**Figures 2–4**). In other words, the sedimentation regime shifted from the Labrador Slope and Rise to entirely on the upper Labrador Shelf (i.e., along-flow transport), in which the Labrador Current was the principal driver in sediment mobilization and meltwater distribution during the Holocene.

4.2 Contrasting Sedimentation Style Between H1, H2, and H4, and H3 Layers in the Labrador Sea

Sedimentary structures and thicknesses of H layers reflect different sedimentation styles, implying close iceberg rafting, sediment transport, and plume interaction. **Figures 2–7** provide documentation of such interactions on the vast Labrador Shelf, Slope, and Basin.

4.2.1 Fine-Grained Sediment Exhaustion due to Long-Distance Transport

Sediment records from the Labrador and NE Newfoundland Shelf stretching >2,000 km from the Hudson Strait to the NE Newfoundland Shelf to SE Grand Banks provide a broad perspective on the sediment dynamics. H1, H2, and H4 layer thicknesses vary from 100 to 400 cm off Hudson Strait (Saglek Bank) and the surrounding region (Andrews et al., 1993; Rashid et al., 2003a; Rashid and Piper, 2007) to 40–60 cm (**Figure 4**; this study) on the Hopedale Saddle to 20–30 cm on the Hamilton Spur (**Figure 5**; this study) to 30–40 cm (Mao et al., 2018) on the northern Flemish Cap slope. Furthermore, near-identical H1, H2, and H4-layer sediment thickness from Flemish Pass (Marshall et al., 2014) and the SE Grand Banks (Rashid et al., 2017; 2019c) were also reported. The typical nepheloid flow layer deposits dominate the variable thickness of H layers (**Figure 7**) found off Hudson Strait and the surrounding regions (Hesse and Khodabakhsh, 1998; Rashid et al., 2003a). However, such a distinction between the nepheloid flow layer deposits and the IRD laminae progressively disappears in the distal region on the northern Flemish Cap slope (Mao et al., 2018) or SE Grand Banks

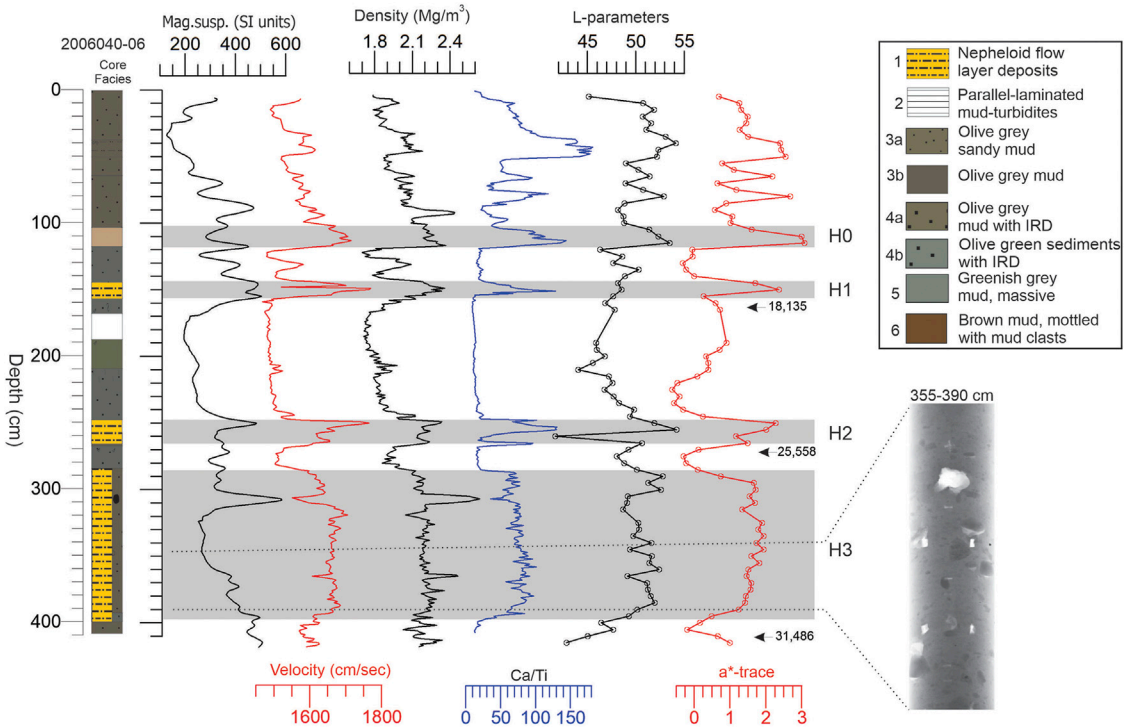

FIGURE 5 | Three sediment physical properties, that is, magnetic susceptibility, P-wave velocity, and density, Ca/Ti ratios, and sediment color L* and a*-traces between the core top and 418 cm subsurface depth of core Hu2006040-06 are plotted. Three ^{14}C-AMS dates were used to confirm the identification of H1, H2, and H3 layers, whereas the X-radiographs and core photographs were used to guide the identification of sedimentary structures and facies shown in column (a). A representative X-radiograph between 355 and 390 cm of H3 layer suggests a near absence of fine-grained plume laminae (suggesting that the Hudson Strait derived fines were depleted on the Hamilton Spur).

(Rashid et al., 2017; Rashid et al., 2019c). As a result, H layers in these distal sites were identified mostly by the IRD layers interspersed with fine to coarse-grained dropstone (**Figure 7**). The disappearance of the distinction between the nepheloid flow layer deposits and the IRD laminae is most likely due to exhaustion (owing to long-distance transport and raining out) of fines in sediment plumes from its source (i.e., Hudson Strait).

In contrast to the H1, H2, and H4 layer, the H3 layer off Hudson Strait (33), southern Saglek Bank (47), Nain Bank (58), and Hamilton Bank (06) of the Labrador Shelf shows distinct sediment facies. Proximal to the Hudson Strait, H3 sediment facies is identified by a combination of fine-grained carbonate-rich mud turbidites underlain by tens of centimeters thick nepheloid flow layer deposits. However, on the Nain Bank (**Figure 4**) and Hamilton Bank (**Figure 5**), the H3 layer is only identified by the nepheloid flow layer deposits in which the distinction (demarcation) between the fine-grained turbidities is nearly absent (**Figure 7**). This difference in sediment facies in proximal vs. relatively distal sites for the same H3 layer most likely suggests 1) the impact of the Coriolis force in guiding sediment plume along the Labrador margin toward the equator. It is hypothesized that the Coriolis force guided the freshwater and sediment plume to flow along the Labrador coast following the shallow bathymetry. Using a numerical model, Chapman (2000) simulated the boundary layer control of buoyant Labrador coastal currents and the establishment of a shelf break front of modern freshwater transport, which we refer to as a corollary to H events. Furthermore, the difference in sediment facies suggests that 2) raining out of the relatively coarse particles (i.e., coarse silt) from sediment plumes through their journey from the Hudson Strait source. However, the deposition of IRD layers simply suggests continuous supply and transport of icebergs laden with IRD, which did not run out.

4.2.2 Nepheloid Flow Layer Deposits and Mass Transport Deposits Mix

Hudson Strait and its surrounding regions on Labrador Slope and Rise sites show two different sediment facies (**Figures 2**, **3**, **7**). H1, H2, and H4 layers are characterized by the nepheloid flow layer deposits. Contrastingly, the H3 layer shows composite sediment facies in which carbonate-rich fine-grained turbidites top the nepheloid flow layer deposits at the bottom (with or) without the interspersed dropstone (core 34). Hesse et al. (2004) proposed mechanisms by which turbidites could be deposited immediately after the nepheloid flow layer deposits by destabilizing the Labrador Slope sediments. The extent to which the destabilization of upper slope sediments would mechanistically function immediately after the deposition of H layers requires modeling results, which are currently unavailable. In any case, the

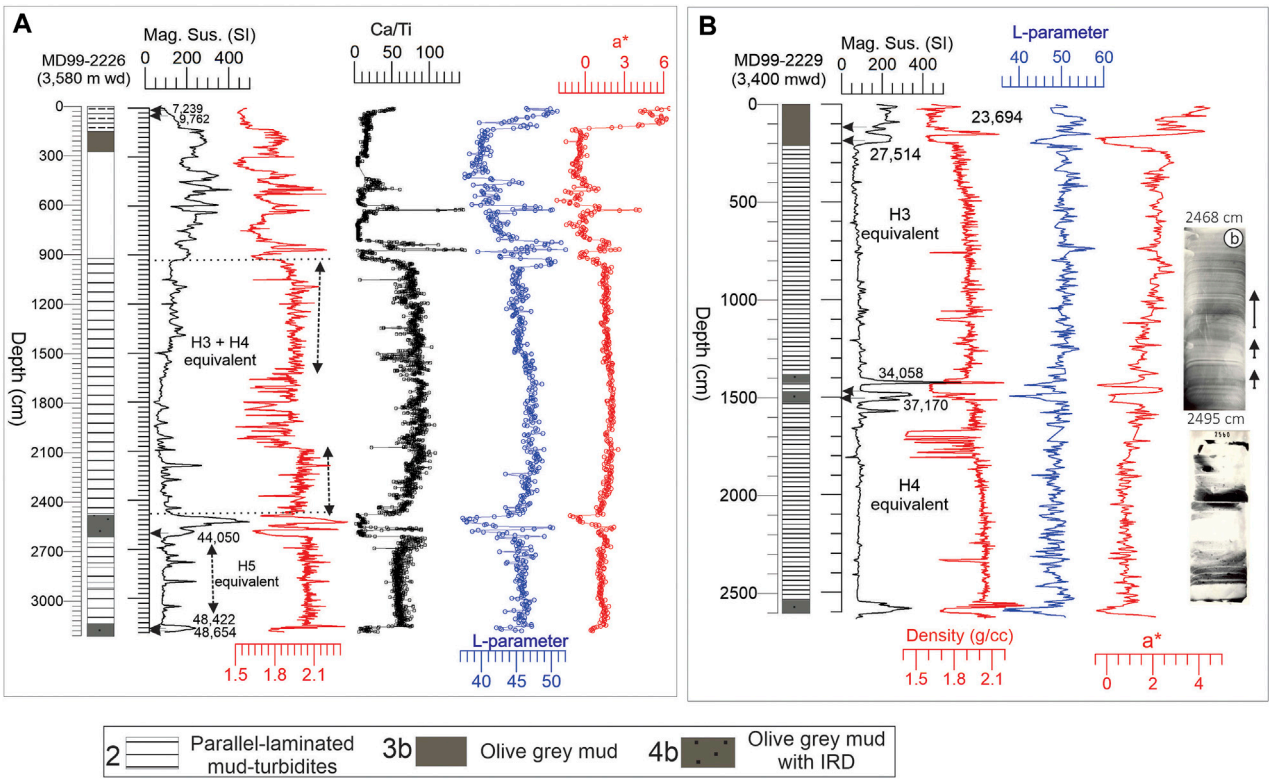

FIGURE 6 | (A) Physical properties (magnetic susceptibility and density) of bulk sediments, Ca/Ti ratios, and sediment color L* and a*-traces of core MD99-2226 are plotted. Five ^{14}C-AMS dates were used to identify H3 and H4 layers. **(B)** Thickness of H3 and H4 layers between 930 and 2595 cm of core MD99-2229 (Cf. Rashid et al., 2019a) is shown to compare with core MD99-2226. X-radiographic images of core MD99-2229 show fine-grained climbing ripple in which coarse silt (dark) and fine silt (white) clay layers irregularly alternate and a typical nepheloid flow layer deposit.

distribution of sediment facies might suggest exertion of Coriolis force in limiting the dispersal of the sediment plume and icebergs rafting as modeled by Chapman (2000) for the modern NW Labrador Sea.

On the lower Labrador Slope and Basin in front of the Hudson Strait, stratigraphically H3 equivalent sediment layer lacks nepheloid flow layer deposits (**Figure 7**), IRD laminae, or dropstones. Rather, the H3 equivalent sediment layer in most of the deepwater cores is identified by thinly laminated carbonate-rich mud turbidites with characteristically laminated silt packages (Rashid et al., 2019a). These H3 mud turbidites are enormously thick and vary from 800 to 1,500 cm (core 08; **Figure 6**), which could be easily traced from off Hudson Strait to >1,800 km distance at site MD95-2023 (core 23) due to their high detrital carbonate (i.e., %$CaCO_3$) content (Hillaire-Marcel et al., 1999; Rashid, 2002). It could be argued that numerous discrete mass transport events all along the Labrador Shelf which evolved into turbidites contributed sediments to site 23 and the adjoining region. The contribution of the Labrador Shelf sediments to site 23 by such a process cannot be completely ruled out; however, the lack of known carbonate sediments or rocks on the Labrador Shelf makes such a proposition unlikely (see Figure 1 of Piper et al., 2021). In any case, the great thickness of turbidites and long-distance transport of the Hudson Strait sourced detrital carbonate-rich sediments suggests: 1) Hudson Strait ice stream had different dynamics compared to the periods of H4 or H2/H1; and 2) sediment destabilization on the Labrador Slope that may have triggered mass transport and deposition on both levees guided by the NAMOC as far distant as site 23 and perhaps beyond (Piper and Hundert, 2002; Rashid et al., 2014). We speculate that there must have been great energy and nature of mud transport deposits due simply to changes in the ice margin in the NE sector of the LIS, as proposed by Dalton et al. (2019).

4.2.3 Deepwater H Event Sedimentation

Sediment remobilization from the NW Labrador Slope and Rise and ensuing mass transport in the deep Labrador Basin during H events have been proposed by Hillaire-Marcel et al. (1994) and Clarke et al. (1999). High-resolution (centimeter-scale intervals) coarse-fraction data from one of the iconic Orphan Knoll cores Hu91045-94 (hereafter 94) show that both H1 and H2 layers have two IRD peaks (Hillaire-Marcel et al., 1994; Stoner et al., 1998; Clarke et al., 1999). The first IRD peak at the base has a proportion of pinkish sand-sized carbonate grains typically exceeding 50% (see **Figure 4**; Clarke et al., 1999), overlain by fine-grained carbonates, which show a sharp increase followed by a gradual decrease. Clarke et al. (1999) proposed that such a pattern reflects both “debris-flow” and “turbidite” deposition rather than iceberg-rafting, with an “initial sorting of the

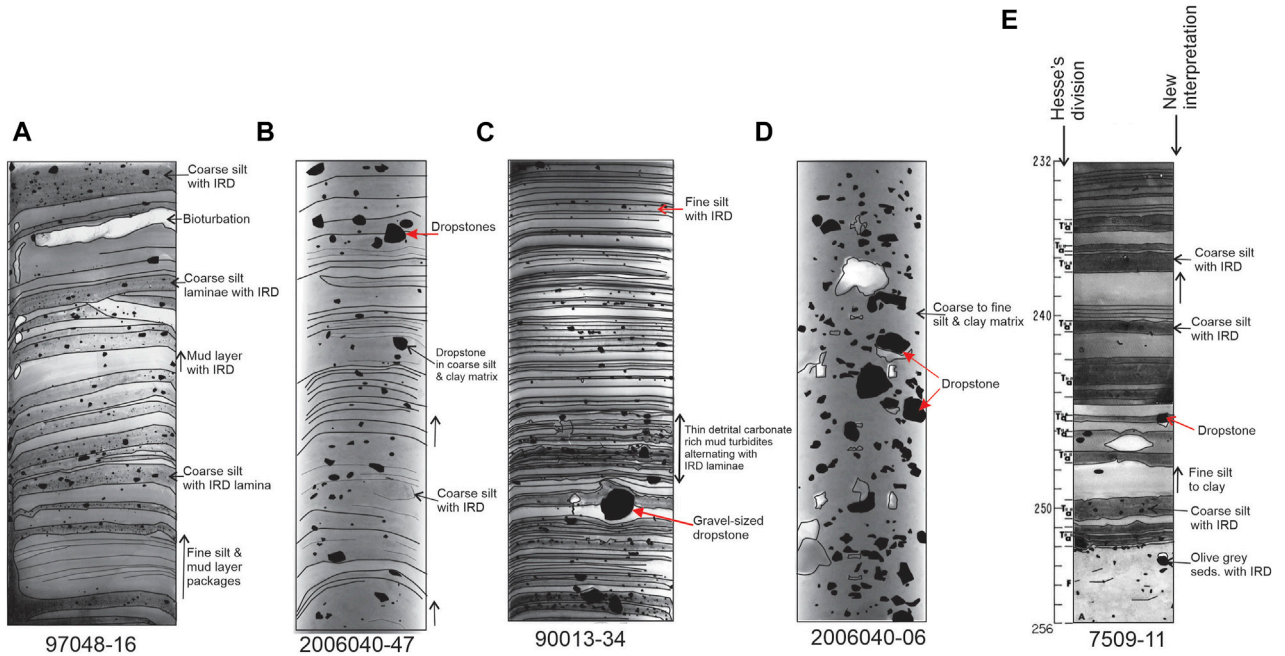

FIGURE 7 | Sedimentary structures derived from the X-radiographs highlight the differences between H3 and other H layers in the Labrador Sea. **(A)** Core Hu97048-16 (H1) shows graded fine silt and mud layers, coarse silt with IRD lamina, and mud layers with occasional IRD or dropstones; **(B)** core Hu2006040-47 (H3) shows dropstones in coarse silt and clay matrix, coarse silt interspersed with IRD with the progressive disappearance of coarse silt with IRD laminae; **(C)** core 90–34 (H3; 255–275 cm) shows thin detrital carbonates rich mud turbidites alternating with IRD laminae, fine silt with IRD and occasional gravel-sized dropstones; and **(D)** core Hu2006040-06 (see also **Figure 5**) shows gravel to pebble-sized dropstones in fine silt and clay matrix. **(E)** reinterpretation of Ta division of turbidite (Hesse et al., 1987) into coarse (dark) silt with IRD, pebble-sized dropstones within the IRD laminae, and mud layer of core Hu75-11 (H2 layer) retrieved from the left levee of the NAMOC (*see* **Figure 1**).

coarse fraction" before the fine-grained carbonate particles accumulate from the turbid cloud (Stoner et al., 1998). The authors further proposed that the silt-sized suspended carbonate sediment was transported by turbidity currents that spilled over from the neighboring NAMOC (Hillaire-Marcel et al., 1994; Hillaire-Marcel and Bilodeau, 2000). Clarke et al. (1999) reported that the second IRD peak at the top shows a substantially reduced proportion of such carbonate grains (~20%) and more silicate grains, which suggests that the IRD in this peak was derived from icebergs of more scattered sources. Such a proposition to invoke both "debris flow" and "turbidite" deposition to explain the IRD peaks during H events is mechanistically impossible in the context of sediment transport considering the bathymetric difference between the NAMOC and the location of core 94 at Orphan Knoll. Furthermore, using a suite of sediment cores from the northern Flemish Cap slope, upslope of core 94, Piper and DeWolfe (2003) and Rashid et al. (2012) demonstrated such typical two IRD peaks during H1 and H2 events. Therefore, to reconcile the inconsistency with this study, an alternative sediment transport mechanism for the deposition of H layers is provided.

First, the proposition that the peak at the base of H1 and H2 (see Figure 4 of Clarke et al., 1999) was deposited by debris flows originating in Hudson Strait, which were guided by and transported along NAMOC to core site 94, could be explained by iceberg calving, rather than by "mass–gravity" flow transport mechanisms. If those coarse-grained materials were to be transported by debris flow, then these deposits could not be considered part of the H layers. If the debris flow were to be originated near the Hudson Strait, it would lose most of the coarse-grained particles owing to the flow evolution on their way to the Orphan Knoll (Lowe, 1976; Shanmugam, 1996). Moreover, the Orphan Knoll site is located on a ridge well above the limit of influence of NAMOC-derived turbidites. There is some evidence of the presence of occasional debris flows derived from slumping on the flanks of Orphan Knoll. However, Huntec high-resolution seismic data from Orphan Knoll (Piper and Campbell, 2005; Tripsanas and Piper, 2008; Huppertz and Piper, 2009) do not show any sign of debris flow around the stratigraphic horizon covered by core 94. In addition, the deposition from the debris flow, which later evolved as turbidity currents, would require merely a few hours to a few days to deposit those fine-grained high carbonates as opposed to the duration of ~800–2,100 years (Veiga-Pires and Hillaire-Marcel, 1999; Elliot et al., 2001; Zhou et al., 2021). Therefore, it is hypothesized that the first IRD peak at the base of H1 is equivalent to the first IRD peak of cores Hu97-16 (see Figure 2 of Rashid et al., 2003b; Rashid et al., 2012) and EW9303-31 (Bond and Lotti, 1995). At the beginning of an H event, icebergs were calved from the Hudson Strait and were transported by the prevailing Labrador Current to the core sites of 94 and Pa96-06 (**Figure 1**), depositing the sandy basal unit.

Second, a thick layer with high fine-grained detrital carbonates above the basal peak in the H layer, equivalent to the nepheloid flow layer deposit found in the NW Labrador Sea and deep Labrador basin cores (Hesse and Khodabakhsh, 1998; Rashid et al., 2003a; Rashid et al., 2019a), is most likely the result of deposition from a turbid plume carried by the prevailing Labrador Current to Flemish Pass and rained down the finer particles from the turbid cloud. This interpretation is consistent with the records from cores Pa96-06 (Rashid et al., 2003a) and Hu2011031-62 (Mao et al., 2018), where the basal IRD peak is overlain by fine-grained carbonate, which does not appear to show any appreciable increase in grain size. Deposition from turbid plumes would require a considerable amount of time, consistent with the duration of H layers at 94 in the Labrador Sea (Veiga-Pires and Hillaire-Marcel, 1999).

Third, the second IRD peak reported for H1 and H2 in core 94 does not show any appreciable increase in the coarse fraction compared to the background level of the coarse fraction of the southern Labrador Sea (Figure 3 of Clarke et al., 1999, p.246). In core Pa96-06, the IRD data do not show any appreciable increase either in comparison to the IRD content of the background sediment (Piper and DeWolfe, 2003; Rashid et al., 2012).

The discussion about mass transport deposits and turbidity currents affords us to address one of the most cited but inaccurate works related to H events in the deep Labrador Basin of Hesse et al. (1987) as well. To increase the clarity and accessibility to a wider audience, we have re-produced one of the X-radiographs of Hesse et al. (1987) of core Hu75-11 (**Figure 7E**). Hesse et al. (1987) reported "a complete sequence of classical Bouma (1962) turbiditic structure divisions, namely, poorly sorted coarse-grained basal division (Ta), followed by parallel (Tb) and cross-laminated divisions (Tc); the thin upper parallel-laminated (Td) which is topped by pelitic division or bioturbated pelagic ooze (F) with ice-rafted debris." Sediment core Hu75-11 was retrieved at 3,625 m water depth on the left levee of the NAMOC, an ideal location to deposit occasional over-spill turbidites. However, a close re-examination of the X-radiograph suggests that the Ta division is simply the IRD layer with coarse silt (dark) as matrix while the fine silt (white) topped it, a common sediment facies found in the NW Labrador Sea cores (**Figures 2**, **3**; see also Figure 4 of Rashid et al., 2003a). Therefore, our reinterpretation of the sequence of sediment layers in H events in core Hu75-11 and the adjacent region requires that icebergs rafting invade the central Labrador Sea.

4.3 Diversity in H3 Sedimentation Between Eastern and Western North Atlantic

A great diversity of data and debate exist regarding the origin and impact of the H3-layer, which divides the open North Atlantic into two regions (**Figure 1C**). The Hudson Strait has long been hypothesized as the primary source of the icebergs for H events by their characteristic signature of an increase in the absolute amount of IRD (and the detrital carbonate) present in the sediment and a decrease in foraminiferal abundance (Bond et al., 1993; Hodell et al., 2008; Rashid et al., 2021; Zhou et al., 2021). However, a foraminiferal depletion but no significant increase in the absolute amount of IRD was observed in the H3 layer in addition to the lower detrital carbonate concentration. The observations led Gwiazda et al. (1996) to propose "reduced surface productivity or dissolution of foraminifera" for H3. Furthermore, the bulk sediments Sr and Nd isotopic composition of the H3 layer indicate a different origin, and the K/Ar ages of the H3-layer fine fraction are similar to those of the background glacial sediment of the NE Atlantic. These variant geochemical signatures suggested to Gwiazda et al. (1996) that the source of iceberg flux responsible for the H3 layer was different to those of H1, H2, and H4 of LIS origin. Furthermore, Revel et al. (1996) proposed that sediments in the H3 layer might have originated from the western European ice sheets due to their similar Sr isotopic compositions compared to the ambient sediments. Using X-ray fluorescence derived Sr/Si and Sr/Ca ratios at the Integrated Ocean Drilling Program Site 1,308, Hodell et al. (2008) also suggested the absence of LIS sourced sediments in H3 in the eastern North Atlantic.

In contrast to the eastern and central North Atlantic (the Mid-Atlantic Ridge (**Figure 1C**) is used as a marker to divide the North Atlantic into two sectors), where high-resolution records of H layers are plenty, the geochemical and petrological data of H layers from the western North Atlantic are relatively scarce. However, a few high-quality petrographic and geochemical data identify H3-layer, like other H events. For example, Bond and Lotti (1995) showed an increase in the detrital carbonates from core 31 that were correlated to the H3 layer. Labeyrie et al. (1999) documented the presence of the H3 layer using the IRD concentration, oxygen isotopes in the planktonic foraminifera, and micropaleontological data from core CH69-K09 (hereafter 09) from the foot of the Newfoundland Slope. Using a suite of cores from the NW Labrador Sea and NW North Atlantic, Rashid et al. (2003a) and Rashid and Grosjean (2006) demonstrated that the Hudson Strait is the source of the iceberg flux responsible for H3, but Hemming (2004) argued that if the Hudson Strait did contribute, it was not the dominant source without providing any data. Recently, Andrews and Voelker (2018) suggested that all H events are primarily sourced from the Hudson Strait, though the degree to which other ice streams might have also contributed has not been satisfactorily addressed. Recently, Rashid et al. (2017) and Rashid et al. (2019c) identified the H3 layer from a suite of SE Grand Banks' sediment cores. Using two cores from the SW Labrador Sea and the Screech seamount of the Newfoundland Basin, Zhou et al. (2021) combined radiochemical and paleontological data to demonstrate the identification of the H layer, including the H3 layer. In summary, the H3 layer is easily identifiable in the NW Atlantic using traditional and exotic proxies in sediment cores. However, the lack of a clear signature for the H3 layer in the eastern North Atlantic (**Figure 1C**) might reflect both 1) glacio-sedimentological conditions in Hudson Strait and the extent of the Hudson Strait ice stream; and 2) the prevailing surface circulation and sea surface temperature conditions were different compared to H1, H2, and H4 in the North Atlantic. Although it cannot be ascertained due to the limited nature of the data used in this study; however, it is hypothesized that the glacio-sedimentological conditions in the Hudson Strait region might

have been the greatest determinant for the ambiguous nature of the H3 layer. In a recent modeling study in which high-amplitude glacial ocean M2 tide at the time of H3 was used, Velay-Vitow et al. (2020) concluded that most of the sedimentological anomalies associated with H3 could be potentially explained by the longer duration of H3 and that eastern-sector ice streams need not necessarily be invoked in any case. The authors further concluded that the H3 instability evolved more gradually and continued over a longer period of time. Our new sedimentological data from the broader Labrador Sea seem to support this hypothesis.

5 SUMMARY

We have documented differences in sedimentation style between the Holocene and last glaciation using sediment cores covering >1,800 km of the eastern Canadian continental margin and the Labrador Basin. Due to the expansion of the late Pleistocene LIS on the Labrador Shelf and Shelf edge, the vast Labrador Shelf appeared to be a sediment-starved depositional environment. The fine-grained sediments, mostly the detrital carbonate together with meltwater and icebergs rafted detritus, were delivered directly on the upper slope by various ice streams of the eastern sector of the LIS, including the Hudson Strait ice stream. Sediments were carried equatorward by the Labrador Current following the bathymetry on the Labrador continental margin.

Heinrich H1, H2, and H4 layers were identified by their typical nepheloid flow layer sediment facies (i.e., alternating coarse silt and clay-sized laminae with thin ice-rafted debris (IRD) interspersed by coarse- to fine-grained dropstone) in conjunction with distinguishing color, Ca/Ti ratios, and sediment physical properties off Hudson Strait and the surrounding region. In contrast to the Hudson Strait proximal sites, H layers were identified only by the IRD layer or interspersed with the IRD with low magnetic susceptibility, high density, and P-wave velocity in the distal sites, namely, on the Hamilton Bank, northern Flemish Cap slope, and SE Grand Banks.

In contrast to the H1, H2, and H4 layers, the H3 layer proximal to the Hudson Strait ice stream is identified by the combination of mass transport (i.e., turbidites) and nepheloid flow layer deposits. However, in the lower Labrador Slope and Basin, the H3 equivalent layer was identified by the thinly laminated carbonate-rich mud turbidites with characteristically laminated silt packages.

At the onset of the Holocene, the upper Labrador Shelf began to receive fine-grained sediments, meltwater, and occasional icebergs. These changes in the sedimentation regime were most likely due to the gradual retreat of the ice margin fleeting glaciers and ice streams in the SE sectors of the LIS. The lack of sediments on most Labrador Shelf is most likely due to sediment remobilization (i.e., winnowing and erosion) by the powerful Labrador Current during the Holocene period.

DATA AVAILABILITY STATEMENT

The raw data supporting the conclusion of this article are http://ed.gdr.nrcan.gc.ca.

AUTHOR CONTRIBUTIONS

Conceptualization: HR; methodology: HR, JH, and AOB; software: RP; validation: AOB, RP, and HR; resources: HR; data curation: AOB and RP; writing—original draft preparation: HR; writing—review and editing: JH, AOB, and RP; visualization: JH; supervision: HR; project administration: HR; and funding acquisition: HR. All the authors have read and agreed to the published version of the manuscript.

FUNDING

This research was funded by the Natural Science Foundation of China, grant numbers 41976056 and 41776064, and the Atlantic Canada Opportunities Agency, grant number 204567. Shanghai Ocean University and the College of the North Atlantic funded the APC.

ACKNOWLEDGMENTS

Part of the study was conducted when the senior author was at the Memorial University of Newfoundland. Samples used in this study were collected by the Marion Dufresne IMAGES 5 and Geological Survey of Canada (Atlantic) cruise #2006040. The authors wish to thank the captain, crew, and laboratory personnel for their support. HR also acknowledges assistance from Kate Jarrett and Jenna Higgins at the Geological Survey of Canada (Atlantic).

REFERENCES

Andrews, J. T., Dyke, A. S., Tedesco, K., and White, J. W. (1993). Meltwater along the Arctic Margin of the Laurentide Ice Sheet (8-12 Ka) : Stable Isotopic Evidence and Implications for Past Salinity Anomalies. *Geol* 21 (10), 881. doi:10.1130/0091-7613(1993)021<0881:matamo>2.3.co;2

Andrews, J. T., Jennings, A. E., Kerwin, M., Kirby, M., Manley, W., Miller, G. H., et al. (1995). A Heinrich-like Event, H-0 (DC-0): Source(s) for Detrital Carbonate in the North Atlantic during the Younger Dryas Chronozone. *Paleoceanography* 10, 943–952. doi:10.1029/95pa01426

Andrews, J. T., and MacLean, B. (2003). Hudson Strait Ice Streams: a Review of Stratigraphy, Chronology and Links with North Atlantic Heinrich Events. *Boreas* 32, 4–17. doi:10.1080/03009480310001010

Andrews, J. T., and Tedesco, K. (1992). Detrital Carbonate-Rich Sediments, Northwestern Labrador Sea: Implications for Ice-Sheet Dynamics and Iceberg Rafting (Heinrich) Events in the North Atlantic. *Geol* 20, 1087–1090. doi:10.1130/0091-7613(1992)020<1087:dcrsnl>2.3.co;2

Andrews, J. T., and Voelker, A. H. L. (2018). "Heinrich Events" (& Sediments): A History of Terminology and Recommendations for Future Usage. *Quat. Sci. Rev.* 187, 31–40. doi:10.1016/j.quascirev.2018.03.017

Barber, D. C., Dyke, A., Hillaire-Marcel, C., Jennings, A. E., Andrews, J. T., Kerwin, M. W., et al. (1999). Forcing of the Cold Event of 8,200 Years Ago by Catastrophic Drainage of Laurentide Lakes. *Nature* 400, 344–348. doi:10.1038/22504

Bassis, J. N., Petersen, S. V., and Mac Cathles, L. (2017). Heinrich Events Triggered by Ocean Forcing and Modulated by Isostatic Adjustment. *Nature* 542 (7641), 332–334. doi:10.1038/nature21069

Bond, G., Broecker, W., Johnsen, S., McManus, J., Labeyrie, L., Jouzel, J., et al. (1993). Correlations between Climate Records from North Atlantic Sediments and Greenland Ice. *Nature* 365 (6442), 143–147. doi:10.1038/365143a0

Bond, G. C., and Lotti, R. (1995). Iceberg Discharges into the North Atlantic on Millennial Time Scales during the Last Glaciation. *Science* 267 (5200), 1005–1010. doi:10.1126/science.267.5200.1005

Bouma, A. H. (1962). *Sedimentology of Some Flysch Deposits: A Graphic Approach to Facies Interpretation*. Elsevier, 168.

Campbell, D. C. (2007). "Regional Geohazard Assessment of the Labrador Margin," in *Geological Survey of Canada Open File # 5473*, 128.

Chapman, D. C. (2000). Boundary Layer Control of Buoyant Coastal Currents and the Establishment of a Shelfbreak Front*. *J. Phys. Oceanogr.* 30, 2941–2955. doi:10.1175/1520-0485(2001)031<2941:blcobc>2.0.co;2

Clarke, G. K. C., Marshall, S. J., Hillaire-Marcel, C., Bilodeau, G., and Veiga-Pires, C. (1999). A Glaciological Perspective on Heinrich Events. *Mech. Glob. Clim. Change millennial time scales* 112, 243–262. doi:10.1029/gm112p0243

Condron, A., and Hill, J. C. (2021). Timing of Iceberg Scours and Massive Ice-Rafting Events in the Subtropical North Atlantic. *Nat. Commun.* 12 (1), 3668–3714. doi:10.1038/s41467-021-23924-0

Cuven, S., Francus, P., and Lamoureux, S. F. (2010). Estimation of Grain Size Variability with Micro X-ray Fluorescence in Laminated Lacustrine Sediments, Cape Bounty, Canadian High Arctic. *J. Paleolimnol.* 44, 803–817. doi:10.1007/s10933-010-9453-1

Dalton, A. S., Finkelstein, S. A., Forman, S. L., Barnett, P. J., and Mitrovica, J. X. (2019). Was the Laurentide Ice Sheet Significantly Reduced during marine Isotope Stage 3? *Geology* 47 (2). doi:10.1130/g45335.1

Dalton, A. S., Gowan, E. J., Mangerud, J., Möller, P., Lunkka, J. P., and Astakhov, V. (2021). Last interglacial (MIS 5e) sea level proxies in the glaciated Northern Hemisphere. *Earth Syst. Sci. Data Discuss.*, 1–74.

Dalton, A. S., Stokes, C. R., and Batchelor, C. L. (2022). Evolution of the Laurentide and Innuitian Ice Sheets Prior to the Last Glacial Maximum (115 Ka to 25 Ka). *Earth-Science Rev.* 224, 103875. doi:10.1016/j.earscirev.2021.103875

Dowdeswell, J. A., Maslin, M. A., Andrews, J. T., and McCave, I. N. (1995). Iceberg Production, Debris Rafting, and the Extent and Thickness of Heinrich Layers (H-1, H-2) in north Atlantic Sediments. *Geol* 23 (4), 301–304. doi:10.1130/0091-7613(1995)023<0297:ipdrat>2.3.co;2

Elliot, M., Labeyrie, L., Dokken, T., and Manthé, S. (2001). Coherent Patterns of Ice-Rafted Debris Deposits in the Nordic Regions during the Last Glacial (10–60 Ka). *Earth Planet. Sci. Lett.* 194 (1-2), 151–163. doi:10.1016/s0012-821x(01)00561-1

Gibb, O. T., Steinhauer, S., Fréchette, B., de Vernal, A., and Hillaire-Marcel, C. (2015). Diachronous Evolution of Sea Surface Conditions in the Labrador Sea and Baffin Bay since the Last Deglaciation. *The Holocene* 25 (12), 1882–1897. doi:10.1177/0959683615591352

Gwiazda, R. H., Hemming, S. R., and Broecker, W. S. (1996). Tracking the Sources of Icebergs with lead Isotopes: The Provenance of Ice-Rafted Debris in Heinrich Layer 2. *Paleoceanography* 11 (1), 77–93. doi:10.1029/95pa03135

Heaton, T. J., Khler, P., Butzin, M., Bard, E., and Skinner, L. C. (2020). Marine20—the marine Radiocarbon Age Calibration Curve (0–55,000 Cal Bp). *Radiocarbon*, 1–42.

Hemming, S. R. (2004). Heinrich Events: Massive Late Pleistocene Detritus Layers of the North Atlantic and Their Global Climate Imprint. *Rev. Geophys.* 42 (1). doi:10.1029/2003rg000128

Hesse, R., Chough, S. K., and Rakofsky, A. (1987). The Northwest Atlantic Mid-ocean Channel of the Labrador Sea. V. Sedimentology of a Giant Deep-Sea Channel. *Can. J. Earth Sci.* 24, 1595–1624. doi:10.1139/e87-155

Hesse, R., and Khodabakhsh, S. (1998). Depositional Facies of Late Pleistocene Heinrich Events in the Labrador Sea. *Geol* 26, 103–106. doi:10.1130/0091-7613(1998)026<0103:dfolph>2.3.co;2

Hesse, R., and Khodabakhsh, S. (2006). Significance of fine-grained Sediment Lofting from Melt-Water Generated Turbidity Currents for the Timing of Glaciomarine Sediment Transport into the Deep Sea. *Sediment. Geology.* 186 (1-2), 1–11. doi:10.1016/j.sedgeo.2005.10.006

Hesse, R., Rashid, H., and Khodabakhsh, S. (2004). Fine-grained Sediment Lofting from Meltwater-Generated Turbidity Currents during Heinrich Events. *Geol* 32 (5), 449–452. doi:10.1130/g20136.1

Hillaire-Marcel, C., De Vernal, A., and Piper, D. J. (2007). Lake Agassiz Final Drainage Event in the Northwest North Atlantic. *Geophys. Res. Lett.* 34 (15).

Hillaire-Marcel, C., and Bilodeau, G. (2000). Instabilities in the Labrador Sea Water Mass Structure during the Last Climatic Cycle. *Can. J. Earth Sci.* 37 (5), 795–809. doi:10.1139/e99-108

Hillaire-Marcel, C., Turon, J. L., and Participants, S. (1999). *IMAGES 5 on Board the Marion Dufresne*. 2nd leg 30 June - 24 July 1999.

Hillaire-Marcel, C., Vernal, A. D., Bilodeau, G., and Wu, G. (1994). Isotope Stratigraphy, Sedimentation Rates, Deep Circulation, and Carbonate Events in the Labrador Sea during the Last ~ 200 Ka. *Can. J. Earth Sci.* 31 (1), 63–89. doi:10.1139/e94-007

Hodell, D. A., Channell, J. E. T., Curtis, J. H., Romero, O. E., and Röhl, U. (2008). Onset of "Hudson Strait" Heinrich Events in the Eastern North Atlantic at the End of the Middle Pleistocene Transition (~640 Ka)? *Paleoceanography* 23, a–n. doi:10.1029/2008PA001591

Hoffman, J. S. (2016). *Ocean Temperature Variability during the Late Pleistocene*. Corvallis, OR, USA: Unpublished Ph. D. thesisOregon State University, 311.

Hoogakker, B. A. A., McCave, I. N., Elderfield, H., Hillaire-Marcel, C., and Simstich, J. (2014). Holocene Climate Variability in the Labrador Sea. *J. Geol. Soc.* 172, 272–277. doi:10.1144/jgs2013-097

Huppertz, T. J., and Piper, D. J. (2009). The Influence of Shelf-Crossing Glaciation on continental Slope Sedimentation, Flemish Pass, Eastern Canadian continental Margin. *Mar. Geology.* 265 (1-2), 67–85. doi:10.1016/j.margeo.2009.06.017

Jennings, A. E., Andrews, J. T., Pearce, C., Wilson, L., and Olfasdottir, S. (2015). Detrital Carbonate Peaks on the Labrador Shelf, a 13 to 7 Ka Template for Freshwater Forcing from the Hudson Strait Outlet of the Laurentide Ice Sheet into the Subpolar Gyre. *Quat. Sci. Rev.* 107, 62–80.

Josenhans, H. W., Zevenhuizen, J., and Klassen, R. A. (1986). The Quaternary Geology of the Labrador Shelf. *Can. J. Earth Sci.* 23, 1190–1213. doi:10.1139/e86-116

Klaucke, I., Hesse, R., and Ryan, W. B. F. (1998). Seismic Stratigraphy of the Northwest Atlantic Mid-ocean Channel: Growth Pattern of a Mid-ocean Channel-Levee Complex. *Mar. Pet. Geology.* 15 (6), 575–585. doi:10.1016/s0264-8172(98)00044-0

Klaücke, I. (1995). "The Submarine Drainage System of the Labrador Sea: Result of Glacial Input from the Laurentide Ice Sheet," in *Unpublished Ph.D. Thesis: Montreal, Quebec, Canada* (McGill University), 248.

Labeyrie, L., Leclaire, H., Waelbroeck, C., Cortijo, E., Duplessy, J.-C., Vidal, L., et al. (1999). "Temporal Variability of the Surface and Deep Waters of the North West Atlantic Ocean at Orbital and Millenial Scales," in *Mechanisms of Global Climate Change at Millennial Time Scales*. Editors P. U. Clark, R. S. Webb, and L. D. Keigwin (American Geophysical Union Monograph), 112, 77–98. doi:10.1029/gm112p0077

Lazier, J. R. N., and Wright, D. G. (1993). Annual Velocity Variations in the Labrador Current. *J. Phys. Oceanogr.* 23, 659–678. doi:10.1175/1520-0485(1993)023<0659:avvitl>2.0.co;2

Lochte, A. A., Schneider, R., Kienast, M., Repschläger, J., Blanz, T., Garbe-Schönberg, D., et al. (2020). Surface and Subsurface Labrador Shelf Water Mass Conditions during the Last 6000 Years. *Clim. Past* 16, 1127–1143. doi:10.5194/cp-16-1127-2020

Lowe, D. R. (1976). Grain Flow and Grain Flow Deposits. *J. Sed. Petro.* 46, 188–199. doi:10.1306/212f6ef1-2b24-11d7-8648000102c1865d

Maclean, B. (2001). Marine Geology of Hudson Strait and Ungava Bay, Eastern Arctic Canada: Late Quaternary Sediments, Depositional Environments, and Late Glacial-Deglacial History Derived from marine and Terrestrial Studies. *Geol. Surv. Can. Bull.* # 566, 198. doi:10.4095/212180

Mao, L., Piper, D. J. W., Saint-Ange, F., and Andrews, J. T. (2018). Labrador Current Fluctuation during the Last Glacial Cycle. *Mar. Geology.* 395, 234–246. doi:10.1016/j.margeo.2017.10.012

Margold, M., Jansen, J. D., Gurinov, A. L., Codilean, A. T., Fink, D., Preusser, F., et al. (2016). Extensive Glaciation in Transbaikalia, Siberia, at the Last Glacial Maximum. *Quat. Sci. Rev.* 132, 161–174. doi:10.1016/j.quascirev.2015.11.018

Margold, M., Stokes, C. R., and Clark, C. D. (2018). Reconciling Records of Ice Streaming and Ice Margin Retreat to Produce a Palaeogeographic Reconstruction of the Deglaciation of the Laurentide Ice Sheet. *Quat. Sci. Rev.* 189, 1–30. doi:10.1016/j.quascirev.2018.03.013

Marshall, N. R., Piper, D. J. W., Saint-Ange, F., and Campbell, D. C. (2014). Late Quaternary History of Contourite Drifts and Variations in Labrador Current Flow,

Flemish Pass, Offshore Eastern Canada. *Geo-mar Lett.* 34, 457–470. doi:10.1007/s00367-014-0377-z

Matero, I. S. O., Gregoire, L. J., Ivanovic, R. F., Tindall, J. C., and Haywood, A. M. (2017). The 8.2 Ka Cooling Event Caused by Laurentide Ice Saddle Collapse. *Earth Planet. Sci. Lett.* 473, 205–214. doi:10.1016/j.epsl.2017.06.011

Piper, D., and Hundert, T. (20022002). Provenance of Distal Sohm Abyssal Plain Sediments: History of Supply from the Wisconsinan Glaciation in Eastern Canada. *Geo-Marine Lett.* 22, 75–85. doi:10.1007/s00367-002-0101-2

Piper, D. J. W., and Campbell, D. C. (2005). "Quaternary Geology of Flemish Pass and its Application to Geohazard Evaluation for Hydrocarbon Development," in *Petroleum Resources and Reservoirs of the Grand Banks, Eastern Canadian Margin: Geological Association of Canada Special Paper 43*. Editors R. N. Hiscott and A. Pulham, 29–43.

Piper, D. J. W., and DeWolfe, M. (2003). Petrographic Evidence from the Eastern Canadian Margin of Shelf-Crossing Glaciations. *Quat. Int.* 99-100, 99–113. doi:10.1016/s1040-6182(02)00115-5

Piper, D. J. W., Li, G., Andrews, J. T., Jennings, A. E., and Robertson, L. (2021). Transport of fine-grained Sediment in Oceanic Currents: Holocene Supply to Sediment Drifts Around Flemish Cap by the Labrador Current. *Mar. Geology.* 436, 106494. doi:10.1016/j.margeo.2021.106494

Rashid, H., Hesse, R., and Piper, D. J. W. (2003b). Distribution, Thickness and Origin of Heinrich Layer 3 in the Labrador Sea. *Earth Planet. Sci. Lett.* 205, 281–293. doi:10.1016/s0012-821x(02)01047-6

Rashid, H., Hesse, R., and Piper, D. J. W. (2003a). Origin of Unusually Thick Heinrich Layers in Ice-Proximal Regions of the north-west Labrador Sea. *Earth Planet. Sci. Lett.* 208, 319–336. doi:10.1016/s0012-821x(03)00030-x

Rashid, H., Lu, Q. Q., Zeng, M., Wang, Y., and Zhang, Z. W. (2021). Sea-Surface Characteristics of the Newfoundland Basin of the Northwest Atlantic Ocean during the Last 145,000 Years: A Study Based on the Sedimentological and Paleontological Proxies. *Appl. Sci.* 11, 3343–3353. doi:10.3390/app11083343

Rashid, H., Mackillop, K., Sherwin, J., Piper, D. J. W., Marche, B., and Vermooten, M. (2017). Slope Instability on a Shallow Contourite-Dominated continental Margin, southeastern Grand banks, Eastern canada. *Mar. Geology.* 393, 203–215. doi:10.1016/j.margeo.2017.01.001

Rashid, H., Piper, D. J., Drapeau, J., Marin, C., and Smith, M. E. (2019a). Sedimentology and History of Sediment Sources to the NW Labrador Sea during the Past Glacial Cycle. *Quat. Sci. Rev.* 221, 17. doi:10.1016/j.quascirev.2019.105880

Rashid, H., and Piper, D. J. (2007). The Extent of Ice on the continental Shelf off Hudson Strait during Heinrich Events 1-3. *Can. J. Earth Sci.* 44 (11), 1537–1549. doi:10.1139/e07-051

Rashid, H., Piper, D. J. W., and Flower, B. P. (2011). The Role of Hudson Strait Outlet in Younger Dryas Sedimentation in the Labrador Sea. *Geophys. Monogr. Ser.* 193, 93–110. doi:10.1029/2010gm001011

Rashid, H., Piper, D. J. W., MacKillop, K., Ouellette, D., Vermooten, M., Muñoz, A., et al. (2019b). Dynamics of Sediments on a Glacially Influenced, Sediment Starved, Current-Swept continental Margin: The SE Grand Banks Slope off Newfoundland. *Mar. Geology.* 408, 67–86. doi:10.1016/j.margeo.2018.11.012

Rashid, H., Piper, D. J. W., Mansfield, C., Saint-Ange, F., and Polyak, L. (2014). Signature of the Gold cove Event (10.2 Ka) in the Labrador Sea. *Quat. Int.* 352 (nov26), 212–221. doi:10.1016/j.quaint.2014.06.063

Rashid, H., Saint-Ange, F., Barber, D. C., Smith, M. E., and Devalia, N. (2012). Fine Scale Sediment Structure and Geochemical Signature between Eastern and Western North Atlantic during Heinrich Events 1 and 2. *Quat. Sci. Rev.* 46, 136–150. doi:10.1016/j.quascirev.2012.04.026

Rashid, H. (2002). "The Deep-Sea Record of Rapid Late Pleistocene Paleoclimate Change and Ice-Sheet Dynamic from the Labrador Sea Sediments," in *Unpubl. Ph.D. Thesis* (Montréal: McGill University).

Rashid, H., Zeng, M., Wang, Y., Ye, X.-X., and Piper, D. J. W. (2019c). *Passive Canadian Margin Sedimentation during the Late Pleistocene: Implications for Submarine Landslides and Geohazards*. American Geophysical Union. Fall Meeting 2019abstract #OS53A-04.

Reimer, P. J., Austin, W. E. N., Bard, E., Bayliss, A., Blackwell, P. G., Ramsey, C. B., et al. (20202020). The INTCAL20 Northern Hemisphere Radiocarbon Age Calibration Curve (0–55 Cal kBP). *Radiocarbon* 62, 1–33. doi:10.1017/rdc.2020.41

Revel, M., Sinko, J. A., Grousset, F. E., and Biscaye, P. E. (1996). Sr and Nd Isotopes as Tracers of North Atlantic Lithic Particles: Paleoclimatic Implications. *Paleoceanography* 11 (1), 95–113. doi:10.1029/95pa03199

Roger, J., Saint-Ange, F., Lajeunesse, P., Duchesne, M. J., and St-Onge, G. (2013). Late Quaternary Glacial History and Meltwater Discharges along the Northeastern Newfoundland Shelf. *Can. J. Earth Sci.* 50, 1178–1194. doi:10.1139/cjes-2013-0096

Saint-Ange, F., Piper, D. J. W., MacKillop, K., Jarrett, K., Higgins, J., and Ledger-Piercey, S. (2013). *Logs of Piston Cores, Deep-Water Labrador Margin*. Geological Survey of Canada Open File #7109, 193.

Seidenkrantz, M. S., Kuijpers, A., Olsen, J., Pearce, C., Lindblom, S., Ploug, J., et al. (2019). Southwest Greenland Shelf Glaciation during MIS 4 More Extensive Than during the Last Glacial Maximum. *Sci. Rep.* 9 (1), 15617–15711. doi:10.1038/s41598-019-51983-3

Shanmugam, G. (1996). High-density Turbidity Currents; Are They sandy Debris Flows? *J. Sediment. Res.* 66 (1), 2–10. doi:10.1306/d426828e-2b26-11d7-8648000102c1865d

Stoner, J. S., Channell, J. E. T., and Hillaire-Marcel, C. (1998). A 200 Ka Geomagnetic Chronostratigraphy for the Labrador Sea: Indirect Correlation of the Sediment Record to SPECMAP. *Earth Planet. Sci. Lett.* 159 (3-4), 165–181. doi:10.1016/s0012-821x(98)00069-7

Tripsanas, E. K., and Piper, D. J. W. (2008). Late Quaternary Stratigraphy and Sedimentology of Orphan basin: Implications for Meltwater Dispersal in the Southern Labrador Sea. *Palaeogeogr. Palaeoclimatol. Palaeoecol.* 260, 521–539. doi:10.1016/j.palaeo.2007.12.016

Veiga-Pires, C. C., and Hillaire-Marcel, C. (1999). U and Th Isotope Constraints on the Duration of Heinrich Events H0-H4 in the southeastern Labrador Sea. *Paleoceanography* 14 (2), 187–199.

Velay-Vitow, J., Peltier, W. R., and Stuhne, G. R. (2020). An Investigation of the Possibility of Non-laurentide Ice Stream Contributions to Heinrich Event 3. *Quat. Res.* 101, 1–13. doi:10.1017/qua.2020.84

Zhou, Y., McManus, J. F., Jacobel, A. W., Costa, K. M., Wang, S., and Alvarez Caraveo, B. (2021). Enhanced Iceberg Discharge in the Western North Atlantic during All Heinrich Events of the Last Glaciation. *Earth Planet. Sci. Lett.* 564, 116910. doi:10.1016/j.epsl.2021.116910

Conflict of Interest: The authors declare that the research was conducted in the absence of any commercial or financial relationships that could be construed as a potential conflict of interest.